

Reaching, Grasping and Re-grasping: Learning Fine Coordinated Motor Skills

Wenbin Hu, Chuanyu Yang, Kai Yuan, Zhibin Li

Abstract—The ability to adapt to uncertainties, recover from failures, and sensori-motor coordination between hand and fingers are essential skills for fully autonomous robotic grasping. In this paper, we use model-free Deep Reinforcement Learning to obtain a unified control policy for controlling the finger actions and the motion of hand to accomplish seamlessly combined tasks of reaching, grasping and re-grasping. We design a task-orientated reward function to guide the policy exploration, analyze and demonstrate the effectiveness of each reward term. To acquire a robust re-grasping motion, we deploy different initial states during training to experience potential failures that the robot would encounter during grasping due to inaccurate perception or disturbances. The performance of learned policy is evaluated on three different tasks: grasping a static target, grasping a dynamic target, and re-grasping. The quality of learned grasping policy is evaluated based on success rates in different scenarios and the recovery time from failures. The results indicate that the learned policy is able to achieve stable grasps of a static or moving object. Moreover, the policy can adapt to new environmental changes on the fly and execute collision-free re-grasp after a failed attempt, even in difficult configurations within a short recovery time.

I. INTRODUCTION

Quick adaption to new changes and recovery from failures are important features for any control policy for real-world robot applications in the future. For this, autonomous grasping is the fundamental capability of many robotic manipulation tasks. However, the combined control of reaching, grasping and re-grasping in a dynamically changing, non-stationary environment remains a challenge.

From the perspective of traditional planning approaches, reaching and grasping are inherently different and usually planned separately and deployed sequentially. For grasping of a moving ball, vision and proximity sensors have been used from a top-view [1]. Marturi et al. developed an approach of planning pre-grasp posture online and tracking a moving object, where the grasp motion was determined by a human operator [2]. Planning of the complete reaching and grasping motion is quite time-consuming and is often implemented in an open-loop or partially reactive controlled manner [3]. Generally, current planning based methods have good results in solving reaching [1] or grasping problem [4] individually, but the switch between controllers is designed manually. As a next-level performance with increased robustness, reaching, grasping and even re-grasping *should be addressed simultaneously in one unified policy*.

All authors are with the Institute for Perception, Action, and Behaviour, School of Informatics, The University of Edinburgh (10 Crichton Street, Edinburgh, EH8 9AB, United Kingdom)
Email: wenbin.hu@ed.ac.uk

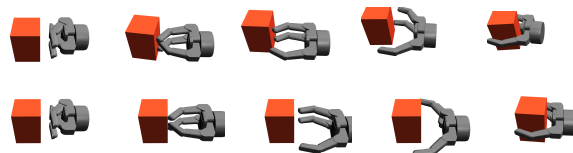


Fig. 1: An example of challenging configuration for re-grasping. Top: undesired re-grasping with collision. Bottom: collision-free re-grasping from our learned policy.

Machine learning methods provide a promising option for autonomous control, as they alleviate the requirements of manual design and prior knowledge as they can autonomously explore the whole operation space and react in potential corner cases. Recently, vision-based data-driven methods show prominent performances [5], [6] in optimization of grasping static objects. Compared with classical grasp synthesis, learning-based approaches improve the performance of grasping unknown objects dramatically [7], [8], [9], [10]. However, training of the model requires very large data, either collected from simulation [7] or self-supervised real robot experiment which is time-consuming [8]. Furthermore, sampling and ranking of grasp candidates often takes long computation time [8], [10], which limits the capability of reactive control. The success of a grasp strongly relies on precise object perception and accurate hardware control. In case of a failure grasp, no recovery strategy is being deployed, and the whole pipeline is simply reset and another attempt is repeated instead of an on-line, reactive adjustment [7].

Recent research in Deep Reinforcement Learning (DRL) has shown promising capabilities of solving continuous control tasks with high-dimensional state and action spaces, such as pouring liquids [11], multi-finger grasping [12], in-hand manipulation [13] or bipedal locomotion tasks [14]. In a Reinforcement Learning framework, an agent learns a policy from scratch by maximizing the expected cumulative return from autonomous interactions with environment. In contrast to other Machine Learning techniques, such as unsupervised and supervised learning, no pre-collected training data is required as the agent autonomously generates the training data by interacting with the environment, and infers the quality of its state and actions through reward signals. Not requiring pre-generated training data is especially useful in large continuous action and state spaces, because labelling whether one action under current state is good or bad is infeasible due to the infinite amount of possible combinations.

The focus of this paper is to study a unified control policy for reaching, grasping and re-grasping, which requires syner-

getic behaviours, fine coordination between hand and fingers. This unified control policy is obtained from training an agent through DRL without any human interference or hard-coded control architecture. Although the task spaces for hand and fingers are different, they have to observe each other’s state and coordinate properly, especially when the hand is approaching the object, otherwise unwanted collision might happen. In this work, we are neither aiming to benchmark with the reaching ability of planning methods nor with the grasp quality of cutting-edge data-driven methods. Instead, we intend to **learn a unified policy with coordinated motor skills for the entire grasping loop**. Most importantly, the **policy should be capable of re-grasping quickly in case of failure**; a problem which has been partially-addressed in aforementioned methods. Real-time failure recovery and re-grasp can significantly increase the robustness and efficiency, and further enable real-world applications, compared to the methods which simply resets the whole pipeline.

The main contributions of this paper are threefold:

- (1) A unified policy of reaching, grasping and re-grasping learned from Deep Reinforcement Learning.
- (2) A task-orientated reward function and special initial states for learning a robust policy.
- (3) Learned policy that is able to achieve robust grasp of static or moving objects, adjust its motion on-line under sudden changes, and re-grasp quickly after failures, even in some difficult configurations as shown in Fig. 1.

In the remainder of this paper, we will firstly discuss the related work in the next section. Then we will elaborate the reinforcement learning algorithm in Section III. Afterwards, the details of the simulation design for policy learning will be presented in Section IV. The results of learned policies will be analyzed and evaluated in Section V. Finally we summarize the paper and propose future work in Section VI.

II. RELATED WORK

Visual servoing methods [15] offer a proper solution to the integration of reaching and grasping. The real-time action is determined by the current vision input, so that the visual servoing methods inherently have the capability of reactive control. However, most applications require large amounts of prior knowledge about the environment and the task [16], or complex hierarchical control architectures [17].

According to the grasping task, force [18] or tactile information [19], [20], [21] has been used as feedback to close the control loop and guide the re-grasping motion. These approaches, however, only modify the applied finger forces or the hand posture for a static target, but are not addressing the problem of handling moving object, or the coordination between hand and fingers.

Some researches solve the reaching and grasping problem through a combination of trajectory planning with policy learning [3] or imitation learning [22]. These methods achieved good results on grasping static novel targets, but the requirements of prior knowledge and hand-crafted control architecture limit the capability of handling environmental changes, such as the sudden movement of the object.

In order to reduce the reliable of knowledge about the system and task’s solution, Lampe et al. [23] combine the classic visual servoing method with DRL. The controller is learned from scratch by success or failure, to control the robot arm to reach and grasp a moving bowl on the table from top-down. The entire combined system is split into two parts: long-range controller mainly for reaching and short-range controller for more precise motion of reaching and grasping. The two controllers are generated differently and use different cameras as vision input. Also, the switch of them is triggered by hand-crafted condition. Compared to [23], instead of manual partition of controller, our approach learns the policy of reaching and grasping in a holistic manner as one policy.

One major deficiency of learning-based grasp detection methods is the long computation time caused by large CNN and individually sampled and ranked grasp candidates [8], [10]. Morrison et al. overcome the problem by proposing a lightweight network structure that enables reactive close-loop control [24]. The learned controller can dynamically track and grasp novel objects in clutter and achieve high success rate. However, this approach has not yet considered the re-grasp problem in case of a failed attempt. In our approach, we introduce challenging configurations that cause failure grasps as additional initial states to train the collision-free re-grasp motion.

III. PRELIMINARIES

In this section we briefly introduce deep reinforcement learning and the proximal policy optimization algorithm that we use for problem formulation and policy learning.

A. Reinforcement Learning(RL)

The task of reaching and grasping an object is considered as a finite-horizon discounted Markov decision process (MDP), consisting of a state space \mathcal{S} , an action space \mathcal{A} , a distribution of initial states $p(s_0)$, the state transition dynamics $\mathcal{T} : \mathcal{S} \times \mathcal{A} \rightarrow \mathcal{S}$, a reward function $r : \mathcal{S} \times \mathcal{A} \rightarrow \mathbb{R}$, and a discount factor $\gamma \in (0, 1]$. Every learning episode starts with a sampled initial state s_0 . Thereafter, at every timestep, the agent chooses one action based on current state and the policy $\pi(s_t)$ to be executed. After execution, the agent will receive a reward $r(s_t, a_t)$ and the state observation s_{t+1} from the environment. The goal of the agent is to maximize the expected discounted sum of rewards $\mathbb{E}_\pi \left[\sum_{t=0}^{T-1} \gamma^t r(s_t, a_t) \right]$.

B. Proximal Policy Optimization(PPO)

In this work, we use an on-policy deep reinforcement learning algorithm named Proximal Policy Optimization (PPO) [25] for policy optimization.

We implement PPO in an actor-critic fashion, with the actor consisting of a policy $\pi_\theta(s_t)$ parameterized by θ and a critic consisting of estimated value function $V_\phi(s_t)$ parameterized by ϕ .

The objective function of PPO is

$$L(\theta) = \hat{\mathbb{E}}_t \left[\min \left(r_t(\theta) \hat{A}_t, \text{clip}(r_t(\theta), 1 - \epsilon, 1 + \epsilon) \hat{A}_t \right) \right], \quad (1)$$

Algorithm 1 Policy learning for dynamic grasping.

```
1: for  $k \in \{1, \dots, N\}$  do
2:   if  $\text{rand}(0, 1) < \beta$  then
3:     Normal initial state with random object position
4:   else
5:     One special initial state in Fig. 5
6:   end if
7:   for  $t \in \{1, \dots, T\}$  do
8:     Get the current state  $\mathcal{S} = \{\mathbf{X}_r, \theta, \mathbf{q}, \mathbf{d}, \mathbf{F}\}$ 
9:     Run policy  $\pi_\theta$  and get the action  $a_t$ 
10:    Execute  $a_t$  based on low-level controller in Fig. 3
11:    Compute reward  $r_t$  with Eq. (3)
12:    Collecting tuple  $\{s_t, a_t, r_t\}$ 
13:  end for
14:   $\pi_{\text{old}} \leftarrow \pi_\theta$ 
15:  Update  $\theta$  by stochastic gradient ascent w.r.t. Eq. (1)
16:  Update  $\phi$  by stochastic gradient descent w.r.t. Eq. (2)
17: end for
```

where $r_t(\theta)$ denotes the probability ratio $\frac{\pi(a_t|s_t)}{\pi_{\text{old}}(a_t|s_t)}$ and \hat{A}_t denotes the estimate of advantage value suggesting whether the action a_t is better or worse than the average action the policy takes at s_t . ϵ is a hyperparameter designed to clip the probability ratio and constrain the policy update. This objective function allows the policy to update towards action distributions with positive advantage while avoiding excessively large policy changes.

The goal of PPO is to maximize the objective function $L(\theta)$, therefore π_θ is updated by gradient ascent w.r.t. Eq. (1). The estimated value function V_ϕ is trained by minimizing the loss function:

$$L(\phi) = \mathbb{E}_t \left[(V(s_t) - R_t)^2 \right], R_t = \sum_{l=0}^{T-t} \gamma^l r_{t+l}, \quad (2)$$

where R_t is the discounted reward during timestep t , γ is the discount factor and T is the total number of timestep during the sampled path. V_ϕ is updated by gradient descent w.r.t. Eq. (2).

Both of the policy π_θ and the value function V_ϕ are parameterized with a fully-connected neural network with two hidden layers of 64 units.

IV. POLICY LEARNING OF DYNAMIC GRASPING

In this section, we present the details for learning a unified policy for reaching, grasping and re-grasping in simulation as demonstrated in Algorithm 1. First, we introduce the simulation environment. Afterwards we describe the control framework. Then, we explain the definition of the state and action space, as well as the design of the reward. Finally, we introduce the structure of training episodes.

A. Simulation Setup

For simulating stable and realistic contacts and dynamics, we use the physics simulation engine MuJoCo [26]. The robot hand used during the policy learning is the Barrett

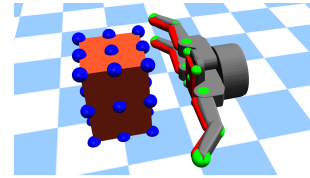


Fig. 2: Floating based Barrett Hand and the target object placed on the ground. Blue points: object geometry key points. Green points: vertexes for forming hand convex hull. Red regions on hand: virtual sites for detecting contact and attaching force sensors.

Hand, which has three fingers, with eight degrees of freedom. The gravity value in simulation is $-9.8m/s^2$

In the simulation environment, the agent will learn the proper motion of the robot hand, including the translational and rotational movement of the hand and the finger actions to accomplish the combined task of reaching, grasping and re-grasping of an object. Since the action space only involves the end-effector, to simplify the environment and learning process, without loss of generality of the proposed approach, we only import the floating based robot hand with realistic, limited moving space and the target object which is placed on the ground in simulation. After the agent learns a good control policy of the hand, the movement of the arm can be obtained through the off-the-shelf inverse kinematics solver and motion planner.

Point cloud has been commonly used to convey object surface information for tasks that involve perception and interaction [27]. In this paper, as a proof of concept, we used a cube as the grasping target. We utilized geometry key points, which can be seen as a sparse point cloud, to encode information of the object. The key points consists of the geometry centre, vertexes, centre of facets and centre of edges of the cube, totalling to 27 points. We assume that the environment is fully observable so that the agent has access to the real-time positions of all the key points. The simulation setup is demonstrated in Fig. 2. Full observation and acquisition of the key point can be achieved with state of the art methods in Computer Vision [28].

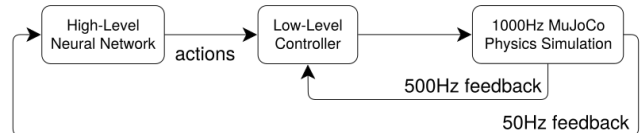


Fig. 3: Block diagram of the control framework.

B. Control Framework

The control framework is designed in a hierarchical architecture, consisting of a high-level and a low-level loop, as shown in Fig. 3. The high-level controller is responsible for producing actions from the output of policy network, based on the current observed environment state, with a frequency of 50Hz. Given the actions output from high-level controller, the 500Hz low-level proportional-derivative (PD) controller is responsible for computing target hand pose and target hand

velocity, as well as the finger joint torques, and feed them into the physics simulation.

C. State and Action Space

We use the term hand as the execution entity for reaching motion and fingers as the entity for grasping. To learn the synergy between hand and fingers, the agent needs to have full awareness of hand and fingers states. Therefore it takes the state $\mathcal{S} = \{X_r, \theta, \mathbf{q}, \mathbf{d}, \mathbf{F}\}$ as input where X_r refers to the three dimensional object position relative to the hand; θ refers to the hand rotation angle around Z axis; \mathbf{q} refers to the three dimensional finger joint angles; \mathbf{d} refers to the distances between each fingertip and the nearest object key point, which we find helpful when the hand is close to the object; \mathbf{F} refers to the seven dimensional contact force measurements. Leveraging contact forces feedback in learning can improve the performance of learned grasp [12]. In simulation, we attach one force sensor on each finger link and one force sensor on the palm. Each sensor will return the magnitude of the contact force.

The grasp detection problem concerns choosing the proper grasp pose and contact points based on the object's shape and that is beyond the scope of this paper. Therefore, to focus on the combined motion of reaching, grasping and re-grasping, we limit the DoF of the end-effector so that it can only approach and grasp the object laterally. We set the palm to always facing the lateral way, and constrain the translational motion of end-effector to the XY two dimensional plane at a certain height. Only the rotation around Z axis is allowed. Hence, the action a consists of the two dimensional translational velocities, rotational velocity around Z axis, and the three dimensional finger torques. The motion of the hand is controlled by the proportional derivative controller.

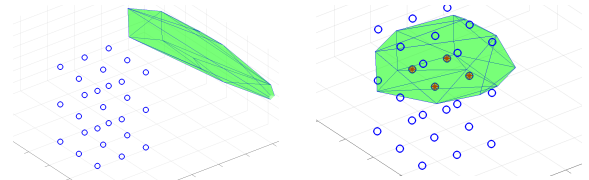
Considering the realism and implementability of the policy in the real world, the working space for end-effector is bounded within a circle at origin with radius of 0.5m. The maximum velocity is bounded within 1m/s and the finger torque is bounded within 2N·m.

D. Reward Design

Reward design is one of the most important aspects in learning a good policy. With a poorly designed reward function, the learning may not converge to the desired policy and may lead to bad performance and safety issues [29]. Reward design is a way to guide the policy search with the researchers' prior knowledge. From experience of how we reach and grasp things like mugs from a table, and observations on how infants learns to reach and grasp, we propose the following reward function, which is the linear combination of multiple positive reward terms and negative penalty terms with corresponding weights $\omega_i, i \in \{1, 2, \dots, 6\}$:

$$r = \omega_1 r_{\text{distTips}} + \omega_2 r_{\text{vector}} + \omega_3 r_{\text{contact}} + \omega_4 r_{\text{topology}} + \omega_5 p_{\text{collision}} + \omega_6 p_{\text{objVel}}, \quad (3)$$

where $(\omega_1, \omega_2, \omega_3, \omega_4, \omega_5, \omega_6) = (1, 1, 2, 10, -1, -2)$. The different terms are computed by the following equations.



(a) Reaching. $r_{\text{topology}} = 0$ (b) Grasping. $r_{\text{topology}} = \frac{4}{27}$

Fig. 4: Visualization of computing the topology reward r_{topology} , in reaching and grasping. Blue points: object geometric key points. Green area: the convex hull formed by key points on hand and fingers. In Fig. 4b four object key points are inside the convex hull.

The term r_{distTips} rewards the distance between the hand and the object, and guides the agent learning to approach the object, where X_i refers to the positions of hand key points - three fingertips and centre of the palm; N_p refers to number of the object key points and Y_j refers to their positions:

$$r_{\text{distTips}} = \exp\left(-\sum_{i=1}^4 \left(\min_{j \in \{1, \dots, N_p\}} \|X_i - Y_j\|\right)\right). \quad (4)$$

In r_{vector} , the vector \vec{U}_i refers to the unit vector pointing from the hand key points to the object geometry centre; \vec{N}_i refers to the normal vector of hand key points. The dot product will lead the hand to learn to face towards the object and grasp it in a proper direction:

$$r_{\text{vector}} = \frac{1}{4} \sum_{i=1}^4 \left(\vec{U}_i \cdot \vec{N}_i\right). \quad (5)$$

In the topology reward r_{topology} , N_p refers to the total number of object key points which is 27; n_{in} refers to the number of points which are inside the three dimensional convex hull formed by the hand and fingers. The convex hull is formed by multiple points including fingertips, finger joints and four corners of the square palm. Fig. 4 shows the convex hull formed by the hand and fingers in reaching and grasping motions:

$$r_{\text{topology}} = \frac{1}{N_p} n_{\text{in}}. \quad (6)$$

In addition to r_{topology} , a contact term r_{contact} is added to encourage power (enveloping) grasping, which is more stable than precision (fingertip) grasp:

$$r_{\text{contact}} = n_{\text{con}}, \quad (7)$$

where n_{con} refers to the number of contact points between object and hand. This term encourages more contact points of the hand with the object during the grasp, under the assumption that with more contact points, the more stable the grasp is. Note that only the contact points in the inner part of hand are counted in n_{con} .

If the hand contacts the object with the outer side of fingers, the contact points are counted in n_c , which is regarded as the penalty term:

$$p_{\text{collision}} = n_c. \quad (8)$$

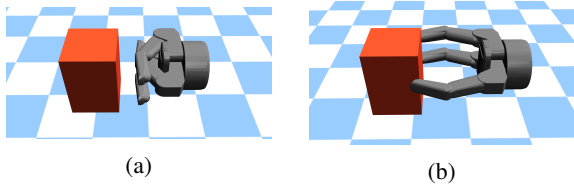


Fig. 5: Two challenging initial states during training: (a) opening fingers without coordination of hand motion would cause collision; (b) shallow, unstable grasp.

A penalty p_{objVel} on the object translational velocity is added to prevent the hand from pushing the object away and encourage a gentle grasping behavior:

$$p_{\text{objVel}} = \|\mathbf{V}_{\text{obj}}\|. \quad (9)$$

E. Learning Episode

A single learning path lasts for 400 time steps in simulation. An episode starts with randomizing the object position, where the cube is being set at a random place on the ground within the operating range. In order to enable the hand to obtain the ability of grasping moving targets, we added random disturbances on the object. The candidate disturbances consist of forces applied on the centre of mass of object in four lateral directions. There is one disturbance duration in each episode, happening at any time in the first half of it, lasting for 0.3 seconds, so the object will slide towards the force direction if not being grasped already.

With randomly added disturbances, the agent can gather enough trials to learn to track and grasp moving target, but it usually fails to achieve the re-grasp motion if the object slips away during the grasp. Randomly distributed disturbance does not provide sufficient data points for the agent to learn the re-grasp. The re-grasp requires synergy motion of fingers and hand. To avoid collision between outer side of fingers and the object, the hand sometimes needs to move backward to make sure there is enough space for opening the fingers. Thus, apart from the normal training episode, we designed three initial states with special finger joints and object position to train the re-grasp policy, as shown in Fig. 5.

V. EVALUATION AND ANALYSIS

In this section, we present the results of the learned policy in simulation, and evaluate the capabilities of reaching, grasping and re-grasping with different metrics and tasks. Moreover, we discuss the necessity and effect of each reward term and initial training states. The evaluation tasks contain: (1) static grasp with random object position; (2) dynamic grasp where a force with random direction would be applied on the object for a certain duration; (3) re-grasp starting from initial configurations shown in Fig. 5a and Fig. 5b and (4) dynamic re-grasp where the object would be moved out of the hand during first grasp attempt.

A. Evaluation Metrics

We evaluate the learned policy with two types of metrics, namely quantitative grasp quality measurement, the success

TABLE I: The evaluation of the policy in different tasks.

	Lift	Shake ₁₂	Shake ₁₅	Recover[s]
Static Target Grasp	97%	90%	69%	∅
Dynamic Grasp(5N, 0.3s)	98%	88%	74%	∅
Dynamic Grasp(8N, 0.3s)	78%	78%	60%	∅
Close Fingers Re-grasp	100%	92%	56%	0.92
Shallow Grasp Re-grasp	100%	100%	91%	0.69
Dynamic Re-grasp	83%	79%	56%	1.48

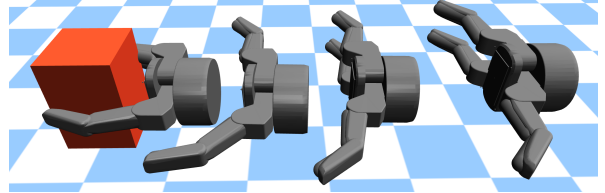


Fig. 6: The reaching and grasping motion of a static object. The hand moves from right to left and grasp the object.

rate in lift and shake tests, and recovery time specially used for re-grasp motion.

In lift test, we will lift the hand, and if the object can be held in the hand for ten seconds, we regard the test as a success. In shake test, we first lift the hand and then apply a force with random direction on the object's CoM. If the object stays in the hand for ten seconds, this test will be marked as a success. Here we set the force to 12N and 15N.

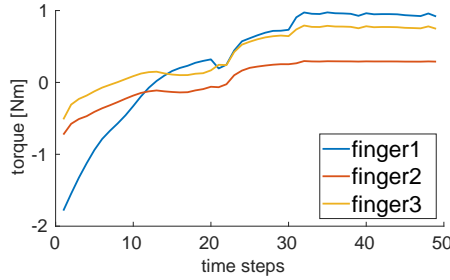
We record the length of the time that the policy spends to recover from the failure and finish a re-grasp attempt. The recovery time is the average shortest time required for the learned agent to achieve a robust grasp which passes the lift and shake tests.

In Table I we present the evaluation of different tasks with different metrics. The results indicate that our approach can generate a robust control policy which can react to changes rapidly and execute re-grasp in case of failures, even under difficult configurations, such as the situations showed in Fig. 5. The achieved grasps are stable for lifting in most cases and can resist external disturbances as shown in the first three columns of Table I.

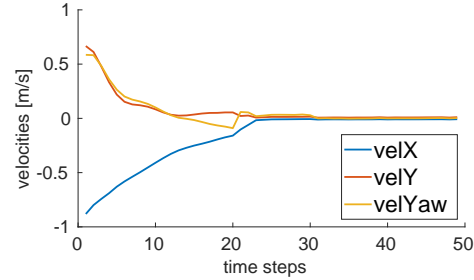
B. Static Target

In this test, the object is placed at a random position, and the task is to reach and grasp it. Fig. 6 demonstrates the reaching and grasping motion generated from the learned policy. The first row of Table I lists the success rates of lift and shake tests which indicates that the learned policy is able to achieve a stable grasp for a static target.

Fig. 7 demonstrates the actions in another typical static grasp task. When the hand is relatively far from the object, the finger torques are negative, which means the fingers are extending and open, enlarging the grasping area. The moving velocity of hand reaches the maximum at the beginning and converge to zero at the end, indicating that the agent learns to slow down when the hand approaches the object. In the end the torque of the first finger is larger than those of the fingers on the opposite side to make the grasp balanced. This behaviour coincides with how humans would grasp an object.



(a) Torque command of each finger.



(b) Translational velocities of the hand.

Fig. 7: The output actions of learned policy during one canonical trial of grasping a static object.

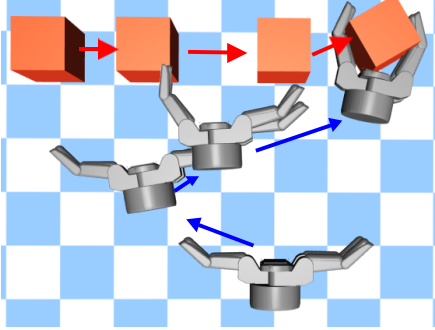


Fig. 8: The time-elapsing snapshots of grasping a moving object. Arrows show moving directions of object and hand.

C. Moving Target

In reinforcement learning, at every control step, the agent takes the current observation of the environment as input and outputs the corresponding actions. Since in this paper the observation only contains object position, the agent has no perception of the object’s motion status such as velocity or acceleration and therefore is unable to predict the object’s future position. Without knowing the object velocity and acceleration, the agent will not be able to learn an optimal policy of grasping a moving object. However, due to the randomization of object position and the disturbances applied on the object during the training, combined with a high enough control frequency. The learned sub-optimal policy has decent tracking capability and is able to dynamically re-adjust to grasp a moving object as long as the object’s velocity is within the agent’s operational velocity.

In this test setting, the object locates at a random position. A force with certain value, pointing to a random direction within the $X - Y$ plane is applied on the object’s CoM for 0.3 second. So the object will start moving at the beginning of the trial. According to Table I, the learned policy is able to adjust online based on the change of object position.

D. Re-grasp Test

In this test setting, in order to evaluate the ability of re-opening the fingers and applying another grasp attempt, the object will be moved out of the hand at the timing when the distance between fingertips and the object is below the threshold. There are two potential consequences. First, the object moves out of the cage formed by fingers and palm

completely. Then the fingers will stop closing and re-open. If the object blocks the fingers from opening, the hand needs to retract backwards to create enough space before re-grasping. In the second situation, the object is caught by the fingertips while moving. This will cause a unstable shallow grasp, so the agent learns to release and re-grasp the object.

Fig. 11 and the second row of Fig. 1 displays the learned re-grasping motions. The agent learns an effective manner to return to a proper pre-grasp posture without any collision and redundant motions. According to the results listed in Table I, the learned policy is able to recover from failures with 2 seconds, which is far more efficient than resetting the whole control pipeline, and achieve a stable grasp which can pass the lift and shake tests with high success rates.

E. Untrained Test Case: Catching

To further validate the effectiveness and the versatility of the trained policy, we created a challenging test scenario (Fig. 9) that was never seen before in the training process. Since the policy was trained in a 2D plane, the robot hand was purposely placed in a vertical plane, where the dimensionality of the problem still holds. The object was launched with an initial velocity being subject to the gravity, creating a projectile trajectory as a flying object.

Despite the test case was not trained explicitly, the learned policy has demonstrated a significant level of generalization towards the successful completion of such a catching task. This suggests that with suitable and sufficient randomisation of initial states, the reactive behaviour learned through training can be versatile and effective for catching a flying object. All videos of snapshots are available in submitted video attachment.

F. Ablation Study

In order to show the necessity and effectiveness of each reward term, we remove them from the reward function, and compare the learned policies with and without it. Fig. 10 demonstrates the learning curves of each reward term, from which we can tell that every term contributes in the policy learning. Table II demonstrates the capabilities of different policies trained with incomplete reward function.

The r_{distTips} and r_{vector} affect the learning first and guide the agent to learn to reach the target. Without r_{distTips} , the hand cannot learn to reach the object. r_{vector} guides the fingers to

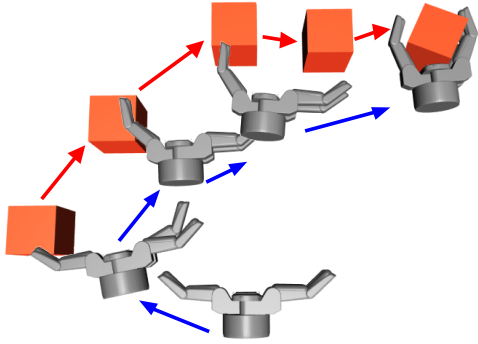


Fig. 9: The catching challenge: an intercepted projectile of a flying object, moving directions are shown by arrows.

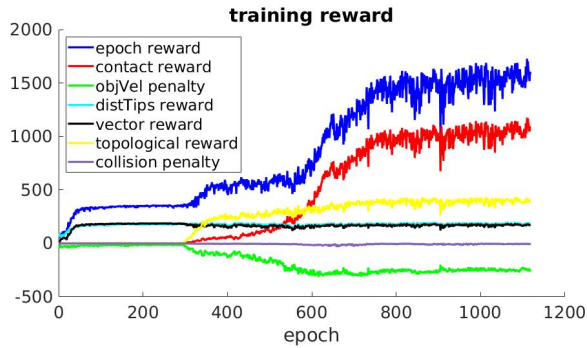


Fig. 10: The learning curves of each reward term in a typical learning process. Each curve represents the sum of the reward term in every epoch. The reward terms in figure are multiplied by the weights in Eq. (3), and the blue curve represents the sum of all reward terms.

keep open when approaching the target. After removing it, the agent fails to learn the proper grasping motion within a certain number of epochs.

The r_{topology} and r_{contact} come to influence afterwards and mainly guide the learning of grasping motion. r_{topology} plays an important role in the early stage of grasping learning when the hand already learned to approach the object. It guides the fingers to wrap around the object, and also compensates the penalty on object velocity caused by the random actions from policy search. After removing r_{topology} in training, the hand learns to stay at a certain distance from the object, with fingers open, in order to avoid the penalty on object velocity. r_{contact} encourages the palm and fingers to contact the object and leads to a firm grasp. After removing r_{contact} , the hand learns to stay at a closer distance from the object and the fingers will form a cage around it, but neither the hand and fingers will contact the object and grasp it.

The penalty on object velocity p_{objVel} is responsible for achieving more gentle grasp motion and preventing the hand from moving the object. The agent can still learn the reaching and grasping motion without this reward term, but the hand will move the object randomly after a successful grasp. The collision penalty $p_{\text{collision}}$ and the three special initial states in Fig. 5 are essential for learning the collision-free re-

TABLE II: Capability tests of policies learned with incomplete reward functions.

	Reach	Grasp	Re-grasp	Lift
No r_{distTips}	✗	✗	✗	✗
No r_{vector}	✓	✗	✗	✗
No r_{topology}	✓	✗	✗	✗
No r_{contact}	✓	✗	✗	✗
No p_{objVel}	✓	✓	✓	✓
No $p_{\text{collision}}$	✓	✓	✗	✓
No special initial states	✓	✓	✗	✓

grasping motion. The first two rows of snapshots in Fig. 1 demonstrate the policies trained with and without the $p_{\text{collision}}$ and initial states. With $p_{\text{collision}}$ and initial states, the hand will move backwards to create enough space for the fingers to open. However, after removing them, the hand will not move backwards and the outer part of fingers will collide with the object while opening.

G. Feasibility of Hardware Experiment

Although the training and evaluation tests are conducted in simulation, we take the realism of generated policy into consideration by discouraging aggressive motions through penalties and bounding the hand velocities and finger torques. Therefore, the difficulty of sim-to-real transfer could be alleviated. Table III displays the peak finger joint torques and hand velocities in different evaluation tasks, each repeated for three times. From the table we can ensure that the motions generated from learned policy are within the boundaries and have enough safety margin. For implementation on different hardware platform, we only need to match the limits used in simulation with those of real robot.

VI. CONCLUSION

In this paper, we used model-free reinforcement learning to acquire the combined control policy of reaching and grasping. In simulation, we used a cube as the target for grasping, a floating based three-fingered robot hand as the end-effector. The agent explores and optimizes the policy through trial-and-error, guided by a well-defined reward function. Apart from the initial learning state with random object configuration, we also incorporate two challenging initial states to train the re-grasping ability by inducing failed attempts. The training results showed that the learned agent can reach and grasp a static target, and also grasp a moving object and generate a collision-free re-grasp after a failure. Through ablation experiments, we demonstrated how each reward term and the special initial states improve the capability and robustness of the learned policy.

As for future work, we will use a real robotic hand mounted on the Franka robot arm to transfer the learned policy from simulation to reality, which is also considered in our training phase as we applied the constraints on the hand motion restricted by the Franka arm. Further research will also be done on robot perception to employ visual feedback into the reinforcement learning framework. In addition, we

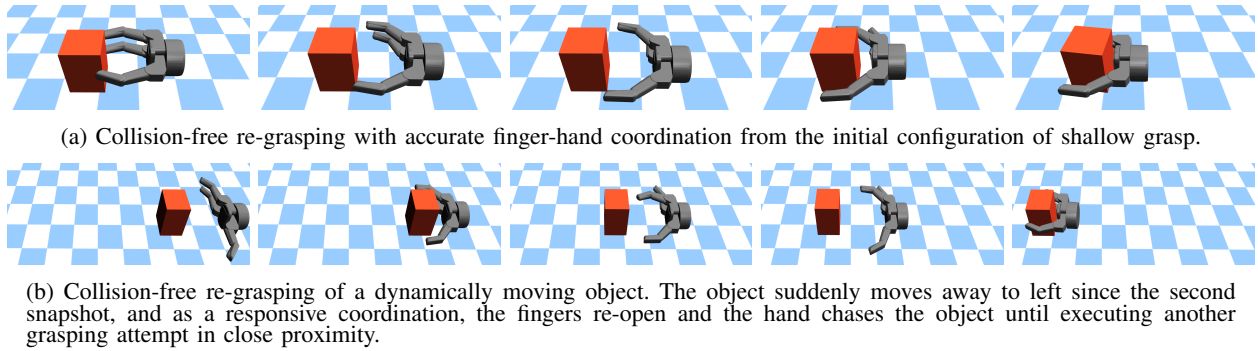


Fig. 11: The snapshots of re-grasping motions generated from the learned policy.

TABLE III: Peak finger torques and hand velocities for different scenarios.

	Peak Finger Joint Torque [$N \cdot m$]			Peak Hand Velocity		
	Finger 1 Base	Finger 2 Base	Finger 3 Base	X [m/s]	Y [m/s]	Yaw [rad/s]
Limit	2	2	2	1	1	1
Static Grasp	1.81	1.01	1.52	0.86	0.81	0.72
Dynamic Grasp(5N, 0.3s)	1.59	0.77	1.08	0.75	1	0.95
Dynamic Grasp(8N, 0.3s)	1.69	0.78	0.96	0.78	0.96	0.81
Close Fingers Re-grasp	1.49	1.91	1.71	0.75	1	0.91
Shallow Grasp Re-grasp	1.12	0.91	0.99	0.81	0.62	0.54

will train the policy with a wide variety of objects to enhance the versatility.

REFERENCES

- [1] Y. Suzuki, K. Koyama, A. Ming, and M. Shimojo, "Grasping strategy for moving object using net-structure proximity sensor and vision sensor," in *2015 IEEE International Conference on Robotics and Automation (ICRA)*, 2015.
- [2] N. Marturi, M. Kopicki, A. Rastegarpanah, V. Rajasekaran, M. Adjigle, R. Stolkin, A. Leonardis, and Y. Bekiroglu, "Dynamic grasp and trajectory planning for moving objects," *Autonomous Robots*, 2019.
- [3] O. Kroemer, R. Detry, J. Piater, and J. Peters, "Combining active learning and reactive control for robot grasping," *Robotics and Autonomous Systems*, 2010.
- [4] K. Hang, J. A. Stork, N. S. Pollard, and D. Kragic, "A framework for optimal grasp contact planning," *IEEE Robotics and Automation Letters*, 2017.
- [5] J. Bohg, A. Morales, T. Asfour, and D. Kragic, "Data-driven grasp synthesis: A survey," *IEEE Transactions on Robotics*, 2014.
- [6] Q. Lu, K. Chenna, B. Sundaralingam, and T. Hermans, "Planning multi-fingered grasps as probabilistic inference in a learned deep network," *CoRR*, 2018.
- [7] D. Kappler, J. Bohg, and S. Schaal, "Leveraging big data for grasp planning," in *2015 IEEE International Conference on Robotics and Automation (ICRA)*, 2015.
- [8] L. Pinto and A. Gupta, "Supersizing self-supervision: Learning to grasp from 50k tries and 700 robot hours," *CoRR*, 2015.
- [9] S. Levine, P. Pastor, A. Krizhevsky, and D. Quillen, "Learning hand-eye coordination for robotic grasping with deep learning and large-scale data collection," *CoRR*, 2016.
- [10] J. Mahler, J. Liang, S. Niyaz, M. Laskey, R. Doan, X. Liu, J. A. Ojea, and K. Goldberg, "Dex-net 2.0: Deep learning to plan robust grasps with synthetic point clouds and analytic grasp metrics," *CoRR*, 2017.
- [11] S. Hangl, E. Ugur, S. Szedmak, J. Piater, and A. Ude, "Reactive, task-specific object manipulation by metric reinforcement learning," in *2015 International Conference on Advanced Robotics (ICAR)*, 2015.
- [12] H. Merzic, M. Bogdanovic, D. Kappler, L. Righetti, and J. Bohg, "Leveraging contact forces for learning to grasp," in *2019 IEEE International Conference on Robotics and Automation (ICRA)*, 2019.
- [13] OpenAI, M. Andrychowicz, B. Baker, M. Chociej, R. Jozefowicz, B. McGrew, J. W. Pachocki, J. Pachocki, A. Petron, M. Plappert, G. Powell, A. Ray, J. Schneider, S. Sidor, J. Tobin, P. Welinder, L. Weng, and W. Zaremba, "Learning dexterous in-hand manipulation," *CoRR*, 2018.
- [14] C. Yang, K. Yuan, W. Merkt, T. Komura, S. Vijayakumar, and Z. Li, "Learning whole-body motor skills for humanoids," in *2018 IEEE-RAS 18th International Conference on Humanoid Robots (Humanoids)*, 2018.
- [15] E. K. Hashimoto, *Visual Servoing: Real-Time Control of Robot Manipulators Based on Visual Sensory Feedback*. World Scientific, 1993.
- [16] W. Hong and J.-J. E. Slotine, "Experiments in hand-eye coordination using active vision," in *Experimental Robotics IV*, O. Khatib and J. K. Salisbury, Eds., 1997.
- [17] A. Namiki, K. Hashimoto, and M. Ishikawa, "A hierarchical control architecture for high-speed visual servoing," *The International Journal of Robotics Research*, 2003.
- [18] P. Pastor, L. Righetti, M. Kalakrishnan, and S. Schaal, "Online movement adaptation based on previous sensor experiences," in *2011 IEEE/RSJ International Conference on Intelligent Robots and Systems*, 2011.
- [19] R. Calandra, A. Owens, D. Jayaraman, J. Lin, W. Yuan, J. Malik, E. H. Adelson, and S. Levine, "More than a feeling: Learning to grasp and regrasp using vision and touch," *CoRR*, 2018.
- [20] F. R. Hogan, M. Bauza, O. Canal, E. Donlon, and A. Rodriguez, "Tactile regrasp: Grasp adjustments via simulated tactile transformations," *CoRR*, 2018.
- [21] Y. Chebotar, K. Hausman, Z. Su, G. S. Sukhatme, and S. Schaal, "Self-supervised regrasping using spatio-temporal tactile features and reinforcement learning," in *2016 IEEE/RSJ International Conference on Intelligent Robots and Systems (IROS)*, 2016.
- [22] N. Ratliff, J. A. Bagnell, and S. S. Srinivasa, "Imitation learning for locomotion and manipulation," in *2007 7th IEEE-RAS International Conference on Humanoid Robots*, 2007.
- [23] T. Lampe and M. Riedmiller, "Acquiring visual servoing reaching and grasping skills using neural reinforcement learning," in *The 2013 International Joint Conference on Neural Networks (IJCNN)*, 2013.
- [24] D. Morrison, P. Corke, and J. Leitner, "Closing the loop for robotic grasping: A real-time, generative grasp synthesis approach," *CoRR*, 2018.
- [25] J. Schulman, F. Wolski, P. Dhariwal, A. Radford, and O. Klimov, "Proximal policy optimization algorithms," *CoRR*, 2017.

- [26] E. Todorov, T. Erez, and Y. Tassa, "Mujoco: A physics engine for model-based control," in *2012 IEEE/RSJ International Conference on Intelligent Robots and Systems*, 2012.
- [27] S. Izadi, D. Kim, O. Hilliges, D. Molyneaux, R. Newcombe, P. Kohli, J. Shotton, S. Hodges, D. Freeman, A. Davison, and A. Fitzgibbon, "Kinectfusion: Real-time 3d reconstruction and interaction using a moving depth camera," in *Proceedings of the 24th Annual ACM Symposium on User Interface Software and Technology*. ACM, 2011.
- [28] X.-F. Han, J. S. Jin, M.-J. Wang, W. Jiang, L. Gao, and L. Xiao, "A review of algorithms for filtering the 3d point cloud," *Signal Processing: Image Communication*, 2017.
- [29] D. Amodei, C. Olah, J. Steinhardt, P. F. Christiano, J. Schulman, and D. Mane, "Concrete problems in AI safety," *CoRR*, 2016.